Atomistic modeling of the (a+c)-mixed dislocation core in wurtzite GaN

I. Belabbas,[1,2,*] A. Béré,[1,4] J. Chen,[3] S. Petit,[1] M. Akli Belkhir,[2] P. Ruterana,[1] and G. Nouet[1]

[1]*Laboratoire Structure des Interfaces et Fonctionnalité des Couches Minces, UMR CNRS 6176, Ecole Nationale Supérieure d'Ingénieurs de Caen, 6 Boulevard du Maréchal Juin, 14050 Caen cedex, France*

[2]*Groupe de Physique du Solide, Laboratoire de Physique Théorique, Université A. Mira de Béjaia, Algeria*

[3]*Laboratoire de Recherche sur les Propriétés des Matériaux Nouveaux, Institut Universitaire de Technologie d'Alençon, 61250 Damigny, France*

[4]*Laboratoire de Physique et de Chimie de l'Environnement, Université de Ouagadougou, 03 BP: 7021 Ouagadougou 03, Burkina Faso*

(Received 6 July 2006; revised manuscript received 15 November 2006; published 6 March 2007)

An atomistic simulation of the threading (**a**+**c**)-mixed dislocation core in wurtzite GaN has been carried out. Starting from models generated in the framework of continuum elasticity theory, two core configurations are obtained independently by using an empirical potential and a tight-binding based *ab initio* method. The most energetically favorable core with a 5/7-atoms ring structure is fully coordinated without wrong bonds, whereas the other with a complex double 5/6-atoms ring structure contains two rows of dangling bonds. Both core configurations introduce empty states spread over the upper half of the band gap.

DOI: 10.1103/PhysRevB.75.115201 PACS number(s): 61.72.Lk, 61.72.Bb, 71.15.Nc

I. INTRODUCTION

Owing to its interesting physical properties,[1] gallium nitride has been used in the fabrication of blue light emitting diodes, high-temperature, and high-power electronic devices.[2] Because of the lack of bulk substrate, this material has been grown heteroepitaxially on sapphire or SiC substrates.[3] The significant lattice mismatch between GaN and the used substrates results in a high density of threading dislocations in the grown layers.[4]

In wurtzite GaN grown in the [0001] direction, threading dislocations are of three types, with Burgers vectors: $1/3\langle 11\bar{2}0\rangle$ (*a* edge), $\langle 0001\rangle$ (*c* screw) and $1/3\langle 11\bar{2}3\rangle$ [(*a*+*c*) mixed].[4] Typically, the majority of these dislocations are *a* edge, whereas the *c* screw usually constitutes the smallest fraction.[5] The density of the (**a**+**c**)-mixed dislocations varies between that of the *a* edge[6] and of the ***c*** screw[5] dislocations depending on the growth conditions.

Over the last decade, a tremendous effort has been going on in order to attain a better understanding of the atomic and electronic structures of dislocations in GaN.[7] Among the threading dislocations, the ***a*** edge was extensively investigated. Three stoichiometric core configurations with 8-, 5/7-, and 4-atoms rings structures were theoretically predicted and experimentally observed.[8] Most of the energetic calculations showed the core with the 5/7-atoms ring structure to be the most energetically favored among the stoichiometric ones.[9,10] However, in a recent investigation, using a multiscale based approach, Lymperakis *et al.* reported the 4-atoms ring core to become the most stable in the presence of tensile strain.[11] Beside the previous core configurations, nonstoichiometric ones have also been theoretically reported[12] and experimentally observed.[13] Their stability was shown to depend both on the growth conditions and charge state.[12]

In spite of their reduced number, the ***c***-screw dislocations have also attracted much interest. This is due mainly to their profound impact on the electronic performances of GaN layers.[14] For the ***c***-screw dislocation, different core structures have been experimentally observed: the full-core, the open-core, and the nonstoichiometric configurations.[8] Initial theoretical calculations[15] showed that the open-core configuration is more energetically favorable than the full core. Recent *ab initio* calculations performed by Northrup[16] revealed that screw dislocations with nonstoichiometric core configurations could be more energetically favorable than those with stoichiometric cores under some growth conditions. Indeed, while the Ga-filled core is predicted to be the most stable configuration under Ga-rich conditions, a nonstoichiometric core structure with Ga (50%) and N (25%) atoms was found more energetically favorable in the N-rich conditions.

In contrast to the above dislocations, there is still a lack of information concerning the core structure of the (**a**+**c**)-mixed dislocation. For the time being, only a picture based on the simple superimposition of an edge and a screw component is usually adopted for its core structure.[17] Even if such a basic model can account for the properties of the mixed dislocation far from its center, it is quite limited in describing the core area where the nonlinear effects are dominant. Furthermore, the superimposition principle obviously fails to describe an eventual change in bonding introduced by the presence of one component (edge or screw) with respect to the other. This is more relevant in compound semiconductors, such as gallium nitride, where states of bonding (Ga-N, Ga-Ga, N-N, or dangling bonds) have very different geometrical and electronic features. Recently, Arslan *et al.*[18] succeeded in providing the first *Z*-contrast image of an (**a**+**c**)-mixed dislocation core. The observed structure was interpreted as a filled core with 8-atoms ring configuration, just like an ***a***-edge dislocation projected along the [0001] direction.

Up to date, no model based on atomistic simulation has yet been provided for the (**a**+**c**)-mixed dislocation core to support the experimental observations. To fill this gap, we report here the first atomistic simulations related to this dislocation core. Starting from models generated in the framework of elasticity theory and by using independently two different atomistic simulation methods: an empirical poten-

tial and a tight-binding based *ab initio* method, we succeeded in obtaining the same core structures. In the following, we show that these core structures cannot be simply described by a superimposition of an edge and screw component. The energetic study was accomplished by combining results from atomistic calculations and continuum elasticity theory. Both empirical potential and tight-binding based *ab initio* calculation favor a fully coordinated core without wrong bonds. Finally, we present and discuss the electronic structures of the two cores. Both were found to induce several empty states in the band gap.

II. COMPUTATIONAL METHODS

In the specific case of the $(\mathbf{a}+\mathbf{c})$-mixed dislocation, the presence of both edge and screw components, combined with the large magnitude of the Burgers vector ($b=6.08$ Å), leads to a strong strain field which is extended far away from the dislocation center. As a consequence, large sized models are required to achieve atomistic simulations of such dislocation cores. In the present study, two numerically expedient methods were applied to perform atomistic simulations. These are, an empirical potential (MSW: modified Stillinger-Weber),[9,19] and an accurate tight-binding based *ab initio* method (SCC-DFTB: self-consistent charge density functional tight binding).[20]

In the original version of the Stillinger-Weber potential (SW),[21] there are: a two-body and a three-body term of the potential energy, which correspond to a pair and pseudo-many-body interaction, respectively. The three-body term represents the angular distortion which is important in the description of deformed structures. This potential is unable to take into account the chemical nature of the bonds. The latter was modified to account for the three different kinds of bonds (i.e., Ga-N, Ga-Ga, and N-N "wrong" bonds) which can take place in gallium nitride.[19] The parameters of the MSW potential were fitted to reproduce the wurtzite GaN experimental lattice parameters and elastic constants, as well as the formation energies of the inversion domain and stacking mismatch boundaries.[22]

The SCC-DFTB method[20] belongs to the family of self-consistent tight-binding methods[23] and may be considered as an approximate density functional scheme. In its total energy expression occurs the two usual tight-binding terms, i.e., the band structure and the short-ranged pair potential. Moreover, based on a second order expansion of the Kohn-Sham energy,[24] a third term has been introduced in order to include Coulomb interactions between charge fluctuations. At large distances, this accounts for long-range electrostatic forces between two point charges and approximately includes self-interaction contributions of a given atom when the charges are located at the same atom. The incorporated self-consistent procedure in this term, at the level of Mulliken charges, allows taking into account charge transfer that could occur in heteronuclear systems. The exchange and correlation contributions to the total energy as well as the ionic core-core repulsion are accounted for in the short-ranged pair potential. The latter is obtained by fitting the total energy to full DFT-LDA based calculations carried out on reference systems.[25] The electronic wave function is expanded in a linear combination of atomic orbitals involving a basis set of *s*, *p*, and *d* confined orbitals. The Hamiltonian and overlap matrix elements are obtained from atom-centered valence electron orbitals and the superposition of neutral atomic potentials, and evaluated within the Slater-Koster two-center approximation.[26]

TABLE I. Experimental and calculated (SCC-DFTB, MSW) lattice parameters and bulk modulus of wurtzite gallium nitride.

	Lattice parameters (Å)	Bulk modulus (GPa)
Experiment	$a=3.190$[a]	188[b]
	$c=5.189$[a]	210[c]
SCC-DFTB	$a=3.178$	189
	$c=5.214$	
MSW	$a=3.190$	209
	$c=5.200$	

[a]Experimental data by Schultz *et al.* (Ref. 28).
[b]Experimental data by Xia *et al.* (Ref. 29).
[c]Experimental data by Polian *et al.* (Ref. 30).

Both the MSW-potential and the SCC-DFTB method were extensively applied to investigate dislocations and grain boundaries in gallium nitride.[8,27] In the present study, we have first carried out test calculations on bulk gallium nitride by using as well the MSW-potential as the SCC-DFTB method. The results are summarized in Table I. The calculated lattice parameters were found to be in good agreement with the experimentally observed values. For the bulk modulus we have obtained values which are in the range of the those provided by experiments. Finally, within the SCC-DFTB method, the evaluation of the Mulliken charges on each atom leads to a charge transfer of $0.56e$ from the Ga to N atoms, resulting in a polar bonding character.

III. SIMULATION MODELS

To perform atomistic simulation of dislocation cores one needs to consider an atomistic model which should reasonably represent the core region, and adopt suitable boundary conditions. Different models were applied for this purpose: supercells, clusters, and supercell-cluster hybrids. In the supercell model,[31] the translational symmetry is artificially restored by applying periodic boundary conditions in the three directions. This imposes to arrange the dislocations in a multipolarlike configuration (dipolar or quadripolar) in order to have zero Burgers vector content. The periodic boundary conditions eliminate the difficulty of treating atoms at the surface of the simulation cell. However, this model suffers from introducing interactions between an infinite number of dislocations. The cluster model[32] is formed by extracting a finite atomic cluster around the defect area of interest, i.e., the dislocation core. As a result, the dislocation line intersects with the surface of the cluster. Although all translational symmetries are lost in this model, it provides at least the ability of treating an isolated dislocation. By using the supercell-cluster hybrid model,[33] one takes advantage of both the supercell and the cluster model. In this approach a single

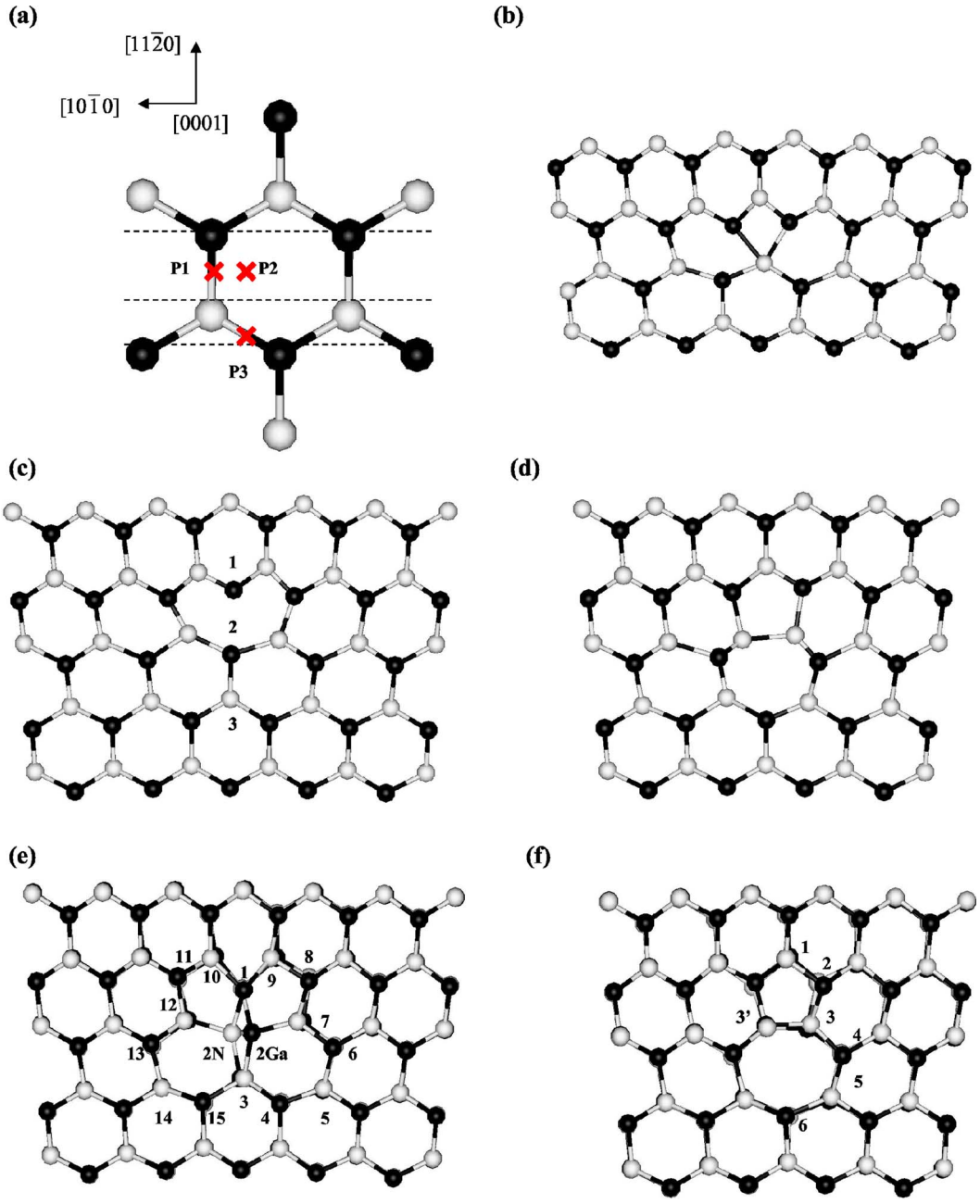

FIG. 1. (Color online) Ball and stick models for starting and relaxed core configurations of the (**a**+**c**)-mixed dislocation. (a): the different origins of the displacement field ($P1$, $P2$, $P3$). (b), (c), and (d): Starting core configurations: 4-atoms ring, 8-atoms ring, and 5/7-atoms ring, corresponding respectively to the origins: $P1$, P,2 and $P3$. (e) and (f): the relaxed core configurations, respectively, the double 5/6- and the 5/7-atoms ring structures. Black balls represent gallium atoms and the white ones nitrogen atoms.

dislocation is treated and besides respecting the natural periodicity of the dislocation along its line direction, it also avoids artificial dislocation-dislocation interactions which occur when a dipole is inserted into a supercell.

In wurtzite GaN, the (**a**+**c**)-mixed threading dislocation lies in the ⟨0001⟩ direction with a $1/3\langle 11\bar{2}3\rangle$ Burgers vector. In all the calculations carried out here, the dislocations were modeled using supercell-cluster hybrids, periodic along the dislocation line direction. The models were constructed as follow: starting from an initial cell with perfect wurtzite GaN structure, a single straight dislocation is introduced by displacing the atoms from their initial positions according to the relations of the displacement field given by linear isotropic elasticity.[34] For this purpose, the expressions suggested by de Wit[35] were adopted as they prevent singularities in the core area. Following Béré *et al.*,[36] different starting core configurations of the dislocation were obtained by changing the position of the origin of the displacement field of the edge component, corresponding to the center of the dislocation, in the two differently spaced $\{10\bar{1}0\}$ prismatic planes [Fig. 1(a)]. The screw component was added to the edge one by conserving the same origin of the displacement field. Similar

to the case of pure edge dislocations, we have obtained by this procedure three initial configurations of the (**a**+**c**)-mixed dislocation. Viewed along the [0001] direction, these core structures look like a 4-, 8-, and 5/7-atoms ring [Figs. 1(b)–1(d)], when the location of the dislocation center is set at: P1, P2, and P3 [Fig. 1(a)], respectively.

In the MSW-potential based calculations, the used models were large rectangular parallelepiped cells with sides along $[11\bar{2}0]$, $[10\bar{1}0]$, and [0001] directions. These models contain 28 800 atoms and their size was $[60a \times 30\sqrt{3}a \times 2c]$ (a and c are the equilibrium lattice parameters). The periodic boundary conditions were applied along the dislocation line direction, while fixed boundaries were imposed perpendicular to the dislocation line. The equilibrium core configurations of the dislocation were obtained by minimising the energy of the supercell-cluster hybrid using quenched molecular dynamics.[37] The equilibrium is reached when the average thermodynamic temperature of the system becomes smaller than 10^{-6} K. For these calculations, we defined two concentric cylinders around the dislocation line, with respective radii of 46 Å and 60 Å, dividing the cell into three parts. The internal region is the area inside the 46 Å radius cylinder, while the external region is the area beyond the 60 Å radius, in between lays the intermediate region. The thickness of both the external and intermediate regions has to be chosen at least larger than the maximum range of the potential (3.36 Å for the Ga-Ga interaction). The atoms in the external region have fixed positions, while those of the internal and intermediate regions are allowed to relax. Eventually, the energy of the system is calculated taking into account only the relaxed atoms in the internal region.

The SCC-DFTB calculations are carried out on hydrogen terminated supercell-cluster hybrids of 764 $(Ga_{320},N_{320},H_{62}^{1.25},H_{62}^{0.75})$ and 760 $(Ga_{318},N_{318},H_{62}^{1.25},H_{62}^{0.75})$ atoms. These were constructed by extracting, from the initial large cells, clusters with about 15 Å of lateral extension around the dislocation line. Pseudohydrogen atoms with fractional charge of $1.25e$ ($0.75e$) were used to cap the Ga (N) dangling bonds at the cluster lateral surface.[38] This procedure allows an emulation of the crystalline bulk by avoiding electronic gap states associated with termination dangling bonds, and as well as surface reconstruction which might induce artificial strain in the dislocation core. The structural relaxations were performed using the conjugate gradient algorithm. For these calculations, the Brillouin zone is sampled only at the Γ point. Within this approximation, the lateral extent of the used models, i.e., perpendicular to the dislocation line direction, is sufficient. However, doubling the size of the models along the dislocation line direction was necessary to obtain total energies that are properly converged. Periodic boundary conditions were applied in the three directions and, following Blumenau *et al.*,[39] the cluster lateral surface was allowed to relax freely. In order to prevent interactions between the supercell-cluster hybrid and those of the neighboring image cells, 190 a.u. thick of vacuum has been only included in the directions perpendicular to the dislocation line. The equilibrium was reached when the atomic forces were below to 0.001 a.u. Finally, the Ga ($3d$) electrons are treated as part of the valence band.[22,40] Since Ga ($3d$) and N ($2s$) orbitals are hybridized, the last consideration may improve the evaluation of the Ga-N bond energy, thus providing more accurate values for the dislocation core energies.

IV. CORE CONFIGURATIONS AND ATOMIC STRUCTURES

Starting from models generated in the framework of linear isotropic elasticity theory [Figs. 1(b)–1(d)], geometry optimisations based on both the MSW potential or the SCC-DFTB method gave similar core structures for the (**a**+**c**)-mixed dislocation. While the configuration with the 5/7-atoms ring structure was conserved [Figs. 1(d) and 1(f)], the initial core configuration with an 8-atoms ring structure [Fig. 1(c)] led to a core with a complex double 5/6-atoms ring structure [Fig. 1(e)]. The initial core with a 4-atoms ring structure [Fig. 1(b)] was found to be unstable, as it turns spontaneously during relaxation to an 8-atoms ring to finally give rise to a double 5/6-atoms ring structure.

In the the 5/7-atoms ring configuration, all the atoms are fully coordinated and they establish only Ga-N bonds [Fig. 1(f)]. This is in contrast to the 5/7-atoms ring core configuration of a pure edge dislocation where wrong bonds (N-N or Ga-Ga) are involved.[41] This change in bonding between a pure edge and a mixed dislocation, is explained as follow: in the presence of only an edge component, each Ga or N atom from the column (3) is at the same level with similar one from the column (3′). However, due to the screw component a relative displacement of $c/2$ is imposed, along the [0001] direction, to the atoms of the latter columns, allowing the formation of Ga-N bonds instead of wrong bonds.

The complex structure of the double 5/6-atoms ring configuration [Fig. 1(e)] may be seen as the result of a strong coupling between the edge and screw components inside the core of the (**a**+**c**)-mixed dislocation. Indeed, in such a configuration there is a presence of profound changes in bonding state with respect to the initial 8-atoms ring core [Fig. 1(c)]. The formation of the double 5/6-atom ring core could be summarized by the following: starting from an 8-atoms ring configuration [Fig. 1(c)], the displacement along the [0001] direction introduced by the screw component enables establishing Ga-N bonds between the atoms of column (1) and those of column (2). As a consequence, a separation of species occurs in the column (2), leading to its splitting into two close subcolumns 2-N and 2-Ga, which are respectively composed only by N and Ga atoms [Fig. 1(e)]. This last effect leads to the occurrence of Ga and N dangling bonds in the columns (7) and (12), respectively.

From the previous analysis, it clearly appears that a simple model based on the superimposition of a screw and an edge component is not adequate in describing the core structure of the (**a**+**c**)-mixed dislocation. Such basic assumption is unable to take into account the changes in the bonding state and their related reconstructions that occur in both the 5/7-atoms ring and the double 5/6-atoms ring cores.

In bulk wurtzite GaN, the equilibrium bond length is 1.95 Å and the equilibrium bond angle, corresponding to sp^3

hybridization, is equal to 109.5°. To our knowledge there are few experimental reports on the atomic structure of the (**a**+**c**)-mixed dislocation core. Recently, by using high resolution transmission electron microscopy (HRTEM), Wang *et al.*[6] attempted to estimate the bond distortions in the vicinity of the (**a**+**c**)-mixed dislocation core. They found the relative bond extension to be in average 6±4% and the relative bond compression to be 7±4%. In the present work, quantitative analysis of the atomic core structure was achieved by calculating the lengths and angles of the different bonds established at particular sites.

A large bond angle dispersion was obtained in the symmetric 5/7-atoms ring core: from 87° to 129° (SCC-DFTB) and from 81° to 135° (MSW). Otherwise, while the most constricted bonds are involved between the Ga atoms at the column (1) and the N atoms at the column (2), −5.81% (SCC-DFTB) or −2.82% (MSW), the most stretched ones are established by the Ga atoms at the column (5) and the N atoms at the column (6), +18.86% (SCC-DFTB) or +12.74% (MSW). In contrast to the 5/7-atoms ring of a pure edge dislocation, where the atoms of the 5-atoms ring involve exclusively compressed bonds and those of the 7-atoms ring exclusively stretched bonds, those of the (**a**+**c**)-mixed dislocation contain atoms with both constricted and stretched bonds, which is attributed to the presence of the screw component. The distance between the two columns, involving Ga-N bonds, separating the two rings of 5 atoms from that with 7 atoms is equal to 1.71 Å (SCC-DFTB) or 1.81 Å (MSW). These values are in between the lengths of the in plane N-N bonds, 1.62 Å (SCC-DFTB) or 1.65 Å (MSW), and the Ga-Ga bonds, 2.26 Å (SCC-DFTB) or 2.24 Å (MSW), established by the atoms belonging to the equivalent columns in the pure edge core.

In the core with a double 5/6-atoms ring structure, the presence of different types of dangling bonds in each side (columns 7 and 12) causes local relaxations that lead to a structural asymmetry. Our calculations show wider bond angle dispersion than that occurs in the 5/7-atoms ring core: from 86° to 134° (SCC-DFTB) and from 77° to 132° (MSW). The most compressed bonds, −8.91% (SCC-DFTB) and −2.67% (MSW), were found to be established by the atoms at columns (7) and (12) that contained dangling bonds. Compressed bonds have also been found to be formed between the two subcolumns 2-Ga and 2-N, −6.95% (SCC-DFTB) and −2.47% (MSW), leading to a separation of 0.76 Å (SCC-DFTB) or 0.85 Å (MSW). Due to the presence of bonds between the previous two subcolumns (2-Ga and 2-N) and both the upper and lower columns (1 and 3), stretched bonds are involved between the atoms belonging to these columns and those of the columns (9) and (10), +15.54% (SCC-DFTB) or +7.50% (MSW), and those of the columns (4) and (15), +11.76% (SCC-DFTB) or +7.44% (MSW).

From the above results, it clearly appears that the values of bond lengths and angles provided by the SCC-DFTB method or the MSW potential are in good agreement for both the double 5/6-atoms ring and the 5/7-atoms ring cores (Tables II and III). However, more stretched bonds are expected in the 5/7-atoms ring core configuration than in the double 5/6-atoms ring one. The cores obtained within the SCC-DFTB method are more strained than those obtained by mean of the MSW potential. Such differences are mainly attributed to the difference in describing the interactions in both methods.

The obtained bond length distortions are more important than those experimentally reported by Wang *et al.*[6] Such difference is attributed to the fact that our calculations are performed in the core itself, while the experimental measurements were made in the core vicinity. Moreover, it is most probable that the lack of a sufficient resolution may not have allowed the above authors to evaluate bond distortions with enough accuracy.

The large stress field produced by the distorted bonds at the (**a**+**c**)-mixed dislocation core is at the origin of attracting impurities and point defects near the dislocation.[42] Moreover, the dangling bonds at the core with a double 5/6-atoms ring structure are expected to be an extra source for attracting impurities. This double 5/6-atoms ring structure can be correlated with the 8-atoms ring structure reported by Arslan *et al.*[18] According to our results, distinguishing a complex double 5/6-atoms ring structure from an 8-atoms ring one requires a subangstrom spatial resolution. Indeed, the major feature of the core with a 5/6-atoms ring structure is the presence of two subcolumns for which the separation was estimated to be between 0.76 and 0.85 Å.

V. ENERGETIC CALCULATIONS

The energetic calculations of the (**a**+**c**)-mixed dislocation cores have been driven by combining continuum elasticity theory and atomistic calculations based on the MSW-potential or SCC-DFTB method. While elasticity theory was used to describe the asymptotic behavior of the dislocation far from its center, the atomistic methods were used to determine the properties of the core area. This procedure allowed us to derive both core energies and radii for the two obtained configurations.

When introduced in a medium, the strain energy (E_{total}) associated with a dislocation is represented as the sum of the elastic ($E_{elastic}$) and core (E_{core}) contributions

$$E_{total} = E_{elastic} + E_{core}. \tag{1}$$

Within linear elasticity, the strain energy per unit length stored in a cylinder of a radius R around the dislocation is given by the relation[34]

$$E_{elastic} = A \ln(R/R_c) \quad \text{for } R > R_c, \tag{2}$$

where R_c is the dislocation core radius.

For a mixed dislocation, the prelogarithmic factor A is related to both the edge and screw components of the Burgers vector (b_e and b_s, respectively) through the relation[34]

$$A = (1/4\pi)(K_e b_e^{\,2} + K_s b_s^{\,2}). \tag{3}$$

The energy factors, K_e and K_s, associated respectively with the edge and screw components, are in the framework of anisotropic elasticity[34]

$$K_e = (C_{11} - C_{12})/2C_{11} \tag{4a}$$

and

TABLE II. Bond lengths (minimum, maximum and average) and bond angles (minimum, maximum and average) at the double 5/6-atoms ring core. The presented values are obtained by the SCC-DFTB method or the MSW potential. For the atom numbers refer to Fig. 1(e).

		Bond lengths (Å)						Bond angles (°)					
	Nature (coordination Nb)	MSW-potential			SCC-DFTB			MSW-potential			SCC-DFTB		
Column		Min	Max	Av	Min	Max	Av	Min	Max	Av	Min	Max	Av
1	Ga (4)	1.98	2.10	2.04	1.90	2.21	2.01	85	122	108	89	117	109
	N (4)	1.98	2.09	2.04	1.90	2.25	2.01	88	123	108	88	118	109
2	Ga (4)	1.90	2.11	2.01	1.82	2.24	2.04	84	131	109	96	131	109
	N (4)	1.90	2.08	1.99	1.81	2.23	2.03	97	130	109	94	129	109
3	Ga (4)	2.03	2.10	2.07	1.99	2.17	2.08	94	123	110	92	123	110
	N (4)	2.03	2.09	2.06	1.99	2.18	2.10	93	122	110	93	122	110
4	Ga (4)	2.00	2.09	2.06	1.98	2.18	2.04	94	119	109	95	118	109
	N (4)	2.00	2.13	2.07	1.98	2.20	2.07	98	123	109	98	121	109
5	Ga (4)	1.94	2.13	2.04	1.91	2.20	2.01	96	120	109	98	121	109
	N (4)	1.99	2.02	2.01	1.95	2.04	1.99	94	123	110	94	122	110
6	Ga (4)	1.93	2.02	1.98	1.89	2.04	1.96	102	121	109	103	123	110
	N (4)	1.93	1.99	1.96	1.85	2.09	1.95	96	123	109	94	123	110
7	Ga (3)	1.90	1.99	1.95	1.78	1.85	1.82	99	123	111	107	126	117
	N (4)	1.93	2.11	2.02	1.84	2.24	2.02	82	132	109	89	133	109
8	Ga (4)	1.92	2.03	1.98	1.84	2.09	1.95	93	123	109	94	123	109
	N (4)	1.90	1.97	1.94	1.78	2.12	1.94	95	126	110	100	122	109
9	Ga (4)	1.93	2.03	1.98	1.86	2.12	1.97	89	129	110	96	134	110
	N (4)	1.92	2.10	2.01	1.84	2.21	2.00	89	126	108	96	121	109
10	Ga (4)	1.90	2.09	2.00	1.83	2.25	1.99	95	122	108	96	120	109
	N (4)	1.94	1.98	1.96	1.86	2.12	1.95	94	129	110	98	129	110
11	Ga (4)	1.90	1.98	1.94	1.77	2.12	1.94	94	124	110	99	121	110
	N (4)	1.90	2.03	1.97	1.83	2.09	1.95	95	124	109	98	124	109
12	Ga (4)	1.92	2.08	2.00	1.82	2.23	2.00	77	131	108	86	134	109
	N (3)	1.90	1.99	1.95	1.77	1.82	1.80	98	122	109	106	124	114
13	Ga (4)	1.94	1.99	1.97	1.82	2.10	1.95	95	122	110	94	124	110
	N (4)	1.92	2.02	1.97	1.86	2.04	1.96	101	123	110	102	124	109
14	Ga (4)	1.98	2.02	2.00	1.96	2.04	2.00	94	123	110	93	124	110
	N (4)	1.94	2.13	2.04	1.93	2.18	2.01	96	120	109	96	122	109
15	Ga (4)	2.00	2.13	2.07	1.98	2.18	2.07	97	123	109	97	121	109
	N (4)	2.00	2.10	2.05	1.98	2.17	2.05	94	119	110	94	119	109

$$K_s = C_{44}, \tag{4b}$$

where C_{11}, C_{12}, and C_{44} are the elastic constants of the material.

In atomistic calculations, one can define the excess of energy related to a single atom as its difference in energy between the system containing the defect and that with bulk material. Thus, the total strain energy contained in a cylinder of radius R around the dislocation is evaluated by summing the excess of energy related to individual atoms inside this area.

In order to determine the core parameters of the dislocation, i.e., core energy and core radius, the total strain energy, obtained by atomistic calculations based on the SCC-DFTB method or the MSW potential, is plotted versus $\ln(R)$ [Figs. 2(a) and 2(b)]. By fitting the previous data to the analytical relation of the elastic strain energy [Eq. (1)], it is possible to identify the core radius of the dislocation as the value from which the curve starts to be linear.[39] The slope of the linear part gives the value of the prelogarithmic factor A.

Thanks to the large lateral extension of the models used in the MSW-potential calculations, a clear linear behavior has been obtained beyond the core area, in the dislocation strain energy curves [Fig. 2(b)]. However, in the case of the SCC-DFTB calculations [Fig. 2(a)], the linear part of the curves are followed by a quick enhancement of the strain energy. This is due to the predominance of the free surface effects with respect to the elastic behavior of the dislocation in that region. By fitting the linear parts of the strain energy curves, the prelogarithmic factors are evaluated for both configura-

TABLE III. Bond lengths (minimum, maximum and average) and bond angles (minimum, maximum and average) at the double 5/7-atoms ring core. The presented values are obtained by the SCC-DFTB method or the MSW potential. For the atom numbers refer to Fig. 1(f).

		Bond lengths (Å)						Bond angles (°)					
		MSW-potential			SCC-DFTB			MSW-potential			SCC-DFTB		
Column	Nature (coordination Nb)	Min	Max	Av	Min	Max	Av	Min	Max	Av	Min	Max	Av
1	Ga (4)	1.90	2.04	1.98	1.84	2.20	1.99	83	130	109	87	128	110
	N (4)	1.91	2.04	1.98	1.85	2.18	1.98	85	132	110	91	126	109
2	Ga (4)	1.91	2.04	1.98	1.86	2.25	1.99	81	127	108	89	122	109
	N (4)	1.91	2.03	1.99	1.82	2.20	1.98	89	135	110	94	127	110
3	Ga (4)	1.97	1.98	1.98	1.94	2.01	1.97	87	119	108	90	119	109
	N (4)	1.91	2.04	1.97	1.82	2.25	1.97	99	130	110	99	129	110
4	Ga (4)	1.91	2.09	1.99	1.83	2.21	1.99	98	124	109	99	121	109
	N (4)	1.98	2.02	2.00	1.95	2.02	1.99	91	124	110	93	119	110
5	Ga (4)	1.98	2.20	2.05	1.95	2.32	2.05	89	125	109	93	121	109
	N (4)	2.00	2.10	2.06	1.97	2.21	2.04	85	125	110	91	121	110
6	Ga (4)	1.99	2.20	2.09	1.97	2.31	2.08	84	128	109	90	124	110
	N (4)	1.99	2.20	2.09	1.98	2.32	2.09	83	129	109	90	126	109

tions, the 5/7- and double 5/6-atoms ring, from as well as the MSW potential (A_{fit}^{MSW}=2.15 eV/Å) as from the SCC-DFTB ($A_{fit}^{SCC\text{-}DFTB}$=2.03 eV/Å) calculations. Despite their underestimation, the latter values well agree with the calculated prelogarithmic factor (A_{th}^{exp}=2.25 eV/Å), obtained by replacing the values of experimental elastic constants in [Eq. (1)].[30] Within the SCC-DFTB calculations a core radius of 6.00 Å is determined for the (**a**+**c**)-mixed dislocation. This value corresponds to a core energy of 3.17 eV/Å for the 5/7-atoms ring and to 3.44 eV/Å for the double 5/6-atoms ring configuration. According to the MSW-potential calculations, the core radius was found to be equal to 7.24 Å corresponding to a core energy of 3.12 eV/Å and 3.32 eV/Å for the 5/7-atoms ring and the double 5/6-atoms ring configuration, respectively.

The previous results show that both the SCC-DFTB method and MSW-potential energetically favor a structure with a 5/7-atoms ring over a double 5/6-atoms ring, with asymptotic energy differences of 0.27 eV/Å (SCC-DFTB) and 0.20 eV/Å (MSW), which are maintained in the elastic limit.

VI. ELECTRONIC STRUCTURES

In gallium nitride, threading dislocations are experimentally associated with nonradiative electronic transitions[43] or with high leakage currents.[44] However, an uncertainty still remains with respect to the contribution of the different kinds of threading dislocations, i.e., ***a***-edge, ***c***-screw, or (**a**+**c**)-mixed, to the previous effects. Nevertheless, almost all the experimental observations agree that the ***c***-screw dislocations have more detrimental impact on gate leakage than the others.[14] This well agrees with the calculated electronic structure, where several states were found to be spread over the entire band gap leading to a metalliclike behavior.[16]

The experimental reports on the electric activity of the (**a**+**c**)-mixed dislocation are conflicting. Combining cathodoluminesce with transmission electron microscopy, Yamamoto *et al.*[45] found these dislocations to act as strong nonradiative centers. However, using the same technique, Remmele *et al.*[13] reported a completely opposite behavior. Such a confusing situation is maintained, in one hand, by the absence of an atomistic model for the (**a**+**c**)-mixed dislocation core and, in the other hand, by the disability to separate experimentally the effect of impurities from that of the dislocations themselves. Accurate electronic structures could be, in principle, provided by full *ab initio* calculations. As in the present case, the size of the considered models is out of reach the latter methods, the electronic structure of dislocations was explored via the SCC-DFTB methodology. Over several applications, the latter method has proven to provide electronic structures qualitatively in the agreement with those obtained by more sophisticated *ab initio* methods.[10,32,33]

The calculated electronic structure showed qualitatively similar features for both the 5/7-atoms ring and the double 5/6-atoms ring configurations [Figs. 3(a) and 3(c)], in spite of their difference in the atomic core structure [Figs. 1(e) and 1(f)]. However, we expect the origin of the introduced gap states to be different in the two cores.

Shallow filled states are present below 0.47 eV, above the valence band maximum, for the 5/7-atoms ring core, and they are below 0.67 eV for the double 5/6-atoms ring core. Empty states are spread over the top half of the band gap for both cores. The filled states are separated from the unfilled ones by 1.36 eV, for the 5/7-atoms ring core, and by 1.18 eV, for the double 5/6-atoms ring core. The origin of the gap states introduced by the dislocation cores was obtained by performing LDOS (local density of states) calculations. Figures 3(b) and 3(d) show the LDOS related to the

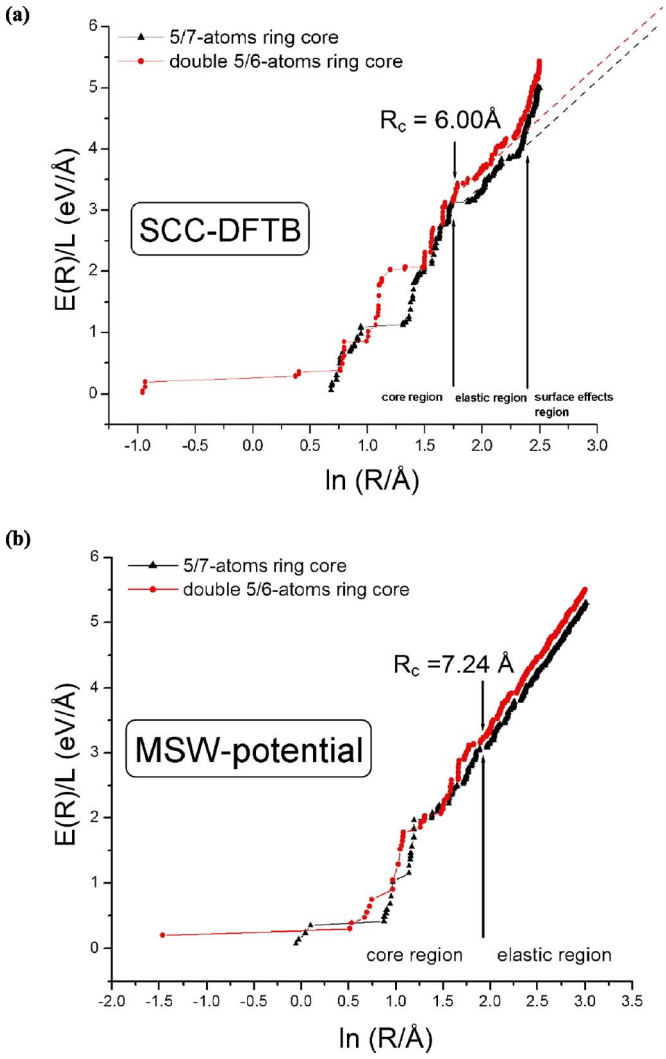

FIG. 2. (Color online) The total strain energy per unit length stored in a cylinder of radius R as a function of $\ln(R)$ for different core configurations of the (**a**+**c**)-mixed dislocation: the double 5/6-atoms ring and the 5/7-atoms ring. (a): The dislocation strain energy calculated by the SCC-DFTB method. The dotted lines represent the asymptotic fit, to the [Eq. (2)], yielding a energy prefactor of 2.03 eV/Å. (b): The dislocation strain energy calculated by the MSW potential.

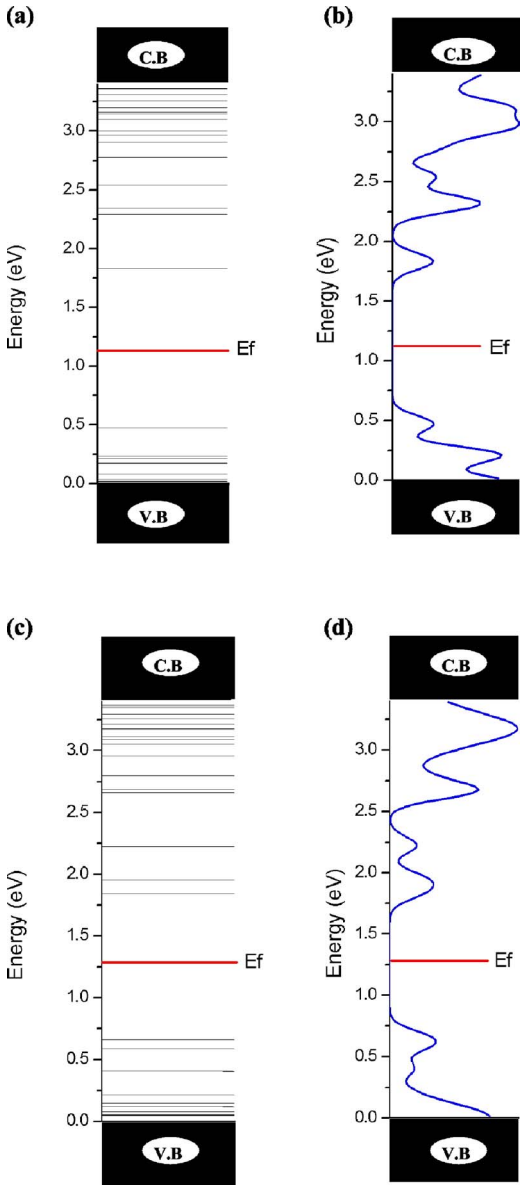

FIG. 3. (Color online) Calculated electronic structures related to the two core configurations, 5/7-atoms ring and double 5/6-atoms ring, of the (**a**+**c**)-mixed dislocation. The zero was put on the top of the valence band maximum while the conduction band minimum is at 3.4 eV. (a): Electronic structure of the dislocation with 5/7-atoms ring structure calculated from the whole model. (b): Local density of states of the dislocation with 5/7-atoms ring structure calculated from the atoms at the core. (c): Electronic structure of the dislocation with double 5/6-atoms ring structure calculated from the whole model. (d): Local density of states of the dislocation with double 5/6-atoms ring structure calculated from the atoms at the core.

core atoms of the 5/7-atoms ring and the double 5/6-atoms ring configurations, respectively. From the comparison of Figs. 3(a), 3(c), 3(b), and 3(d), it comes out that the gap states [Figs. 3(a) and 3(c)] are introduced only by the core atoms [Figs. 3(b) and 3(d)]. Further analysis based on the LDOS calculations showed that both the deepest occupied states, centred around the level $L1$, and the deepest unoccupied sates, centred around the level $L2$, have different origins in the 5/7-atoms ring and in the double 5/6-atoms ring configuration [Figs. 4(a) and 4(b)]. While the states centred around the level $L1$ are contributed from the atoms establishing compressed bonds in the column (1) of 5/7-atoms ring core {Fig. 4(b)], they are due to the N-dangling bonds at the column (12) in the double 5/6-atoms ring core [Fig. 4(a)]. The states centered around the level $L2$ are induced by the atoms involving overstretched bonds between the columns (6) and (5) of the 5/7-atoms ring core [Fig. 4(a)]. However, in the double 5/6-atoms ring core, the previous states are introduced by the Ga-dangling bonds at the column (7) [Fig. 4(b)].

The presence of a high density of empty states in all the top half of the band gap suggests that the (**a**+**c**)-mixed dislocation can be at the origin of nonradiative recombinations.

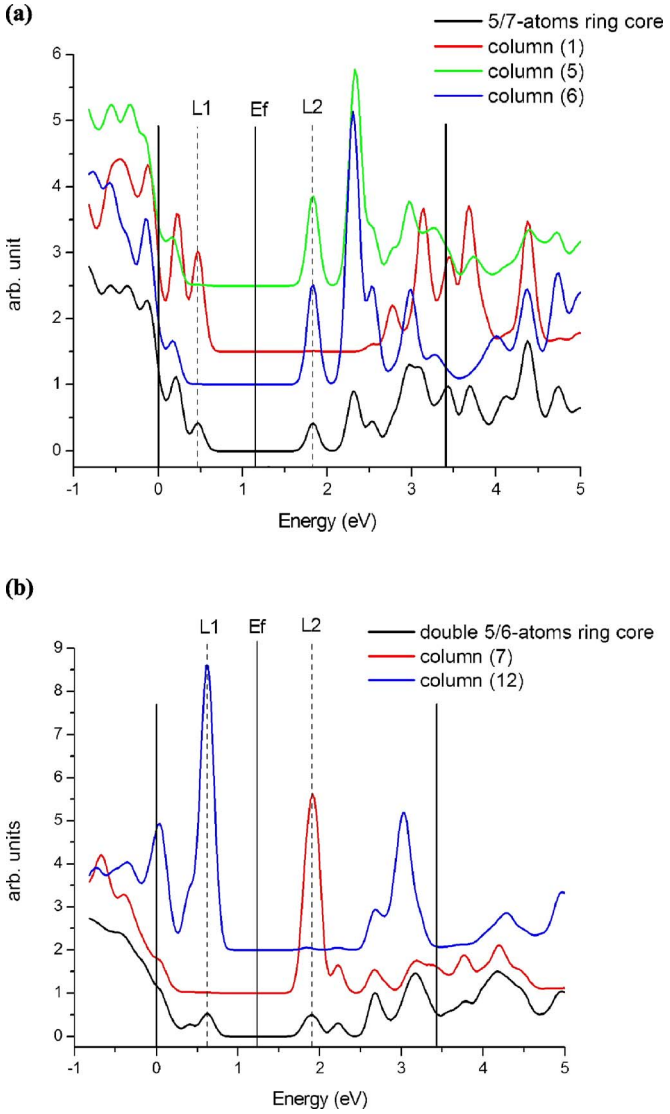

FIG. 4. (Color online) Calculated local density of states representing the contribution of different atomic columns to the deepest occupied states, centred around the level $L1$, and the deepest unoccupied sates, centred around the level $L2$. (a): Local density of states related to particular atomic columns at the 5/7-atoms ring core. (b): Local density of states related to particular atomic columns at the double 5/6-atoms ring core.

However, this activity is expected to be less important than in the case of screw dislocations where the states are spread over the entire band gap.[16] Such behavior is consistent with the experimental observations of Yamamoto *et al.*[45] Otherwise, in *n*-type doped materials, the obtained empty gap states could give rise to a charge migration from the donor atoms, such as silicon and oxygen, to those at the core of $(a+c)$ dislocation.[46] An accumulation of negative charge at threading dislocations has been already observed experimentally.[47] This process allows dislocation cores to act as charged scattering centres leading to a decrease in the carriers mobility.[48]

VII. CONCLUSION

We have performed the first atomistic simulation of the threading (**a**+**c**)-mixed dislocation cores in wurtzite GaN. Our approach is based on a tight-binding based density functional method and a modified Stillinger-Weber potential. Starting from models generated in the frame of linear elasticity theory, the SCC-DFTB method and the MSW-potential lead separately to the same core configurations. These are a 5/7-atoms ring configuration without wrong bonds and a complex double 5/6-atoms ring configuration with two rows of dangling bonds. The energetic calculations have shown the 5/7-atoms ring configuration to be more energetically favorable than the complex double 5/6-atoms ring configuration with both the MSW-potential and SCC-DFTB method.

Our structural analysis has shown that the obtained cores cannot be described by assuming a simple superimposition of the edge and screw components. Indeed, we report fundamental changes in bonding state from initial structures obtained by the superimposition of the previous two components. Severely distorted bonds are established in both cores. The stress field raised from such distortions could be at the origin of a segregation of point defects at the dislocation core. The dangling bonds contained in the core with a double 5/6-atoms ring configuration are an additional source of appeal for impurity segregation. Therefore, this core may be more reactive with impurities than the 5/7-atoms ring configuration. Moreover, the double 5/6-atoms ring core can be related to the 8-atoms ring structure reported by Arslan *et al.* for the (**a**+**c**)-mixed dislocation. According to our results, distinguishing a complex double 5/6-atoms ring structure from an 8-atoms ring one requires a subangstrom spatial resolution. Finally, it was shown that the calculated electronic of the (**a**+**c**)-mixed dislocation was consistent with several experimental observations such as accumulation of negative charges at the dislocation cores and involvement in nonradiative recombination.

ACKNOWLEDGMENTS

This work was supported by EU Marie Curie RTN Contract No. MRTN-CT-2004-005583 (PARSEM). The computations were performed at "CRIHAN," Centre de Ressources Informatiques de HAute Normandie (http://www.crihan.fr).

*Email address: imad.belabbas@ensicaen.fr

[1] S. Strite, M. E. Lin, and H. Morkoç, Thin Solid Films **231**, 197 (1992).

[2] H. Morkoç, R. Cingo1ani, W. Lambrecht, B. Gil, H. X. Jiang, J. Lin, D. Pavlidis, and K. Shenai, MRS Internet J. Nitride Semicond. Res. **4S1**, G1.2 (1999).

[3] S. C. Jain, M. Willander, J. Narayan, and R. Van Overstraeten, J. Appl. Phys. **87**, 965 (2000).

[4] F. A. Ponce, D. Cherns, W. T. Young, and J. W. Steeds, Appl. Phys. Lett. **69**, 770 (1996).
[5] W. Qian, G. S. Rohrer, M. Skowrnonski, K. Doverspike, L. B. Rowland, and D. K Gaskill, Appl. Phys. Lett. **67**, 2284 (1995).
[6] D. Wang, M. Ichikawa, and S. Yoshida, Philos. Mag. Lett. **82**, 119 (2002).
[7] A. T. Blumenau., C. J. Fall, J. Elsner, R. Jones, M. I. Heggie, and Th. Frauenheim, Phys. Status Solidi C **0**, 1684 (2003).
[8] I. Belabbas, P. Ruterana, J. Chen, and G. Nouet, Philos. Mag. **86**, 2241 (2006).
[9] A. Béré, and A. Serra, Phys. Rev. B **65**, 205323 (2002).
[10] S. M. Lee, M. A. Belkhir, X. Y. Zhu, Y. H. Lee, Y. G. Hwang, and Th. Frauenheim, Phys. Rev. B **61**, 16033 (2000).
[11] L. Lymperakis, J. Neugebauer, M. Albrecht, T. Remmele, and H. P. Strunk, Phys. Rev. Lett. **93**, 196401 (2004).
[12] A. F. Wright and U. Grossner, Appl. Phys. Lett. **73**, 2751 (1998).
[13] T. Remmele, M. Albrecht, H. P. Strunk, A. T. Blumenau, M. I. Heggie, J. Elsner, Th. Frauenheim, H. P. D. Schenk, and P. Gibart, Inst. Phys. Conf. Ser. **169**, 323 (2001).
[14] J. W. P. Hsu, M. J. Manfra, R. J. Molnar, B. Heying, and J. S. Speck, Appl. Phys. Lett. **81**, 79 (2002).
[15] J. Elsner, R. Jones, P. K. Sitch, V. D. Porezag, M. Elstner, Th. Frauenheim, M. I. Heggie, S. Oberg, and P. R. Briddon, Phys. Rev. Lett. **79**, 3672 (1997).
[16] J. E. Northrup, Phys. Rev. B **66**, 045204 (2002).
[17] P. Ruterana, V. Potin, G. Nouet, R. Bonnet, and M. Loubradou, Mater. Sci. Eng., B **59**, 177 (1999).
[18] I. Arslan, A. Bleloch, E. A. Stach, and N. D. Browning, Phys. Rev. Lett. **94**, 025504 (2005).
[19] N. Aichoune, V. Potin, P. Ruterana, A. Hairie, G. Nouet, and E. Paumier, Comput. Mater. Sci. **17**, 380 (2000).
[20] M. Elstner, D. Porezag, G. Jungnickel, J. Elsner, M. Haugk, Th. Frauenheim, S. Suhai, and G. Seifert, Phys. Rev. B **58**, 7260 (1998).
[21] F. H. Stillinger and T. A. Weber, Phys. Rev. B **31**, 5262 (1985).
[22] J. E. Northrup, J. Neugebauer, and L. T. Romano, Phys. Rev. Lett. **77**, 103 (1996).
[23] A. P. Horsfield and A. M. Bratkovsky, J. Phys.: Condens. Matter **12**, R1 (2000).
[24] W. M. Foulkes and R. Haydock, Phys. Rev. B **39**, 12520 (1989).
[25] D. Porezag, Th. Frauenheim, and Th. Kohler, G. Seifert and R. Kaschner, Phys. Rev. B **51**, 12947 (1995).
[26] J. C. Slater and G. F. Koster, Phys. Rev. **94**, 1498 (1954).
[27] A. Béré and A. Serra, Philos. Mag. **86**, 2159 (2006).
[28] H. Schultz and K. H. Thiemann, Solid State Commun. **23**, 815 (1977).
[29] H. Xia, Q. Xia, and A. L. Ruoff, Phys. Rev. B **47**, 12925 (1993).
[30] A. Polian, M. Grimsditch, and J. Grzegory, J. Appl. Phys. **79**, 3343 (1996).
[31] J. R. K. Bigger, D. A. McInnes, A. P. Sutton, M. C. Payne, I. Stich, R. D. King-Smith, D. M. Bird, and L. J. Clarke, Phys. Rev. Lett. **69**, 2224 (1992).
[32] A. T. Blumenau, R. Jones, S. Öberg, P. R. Briddon, and Th. Frauenheim, Phys. Rev. Lett. **87**, 187404 (2001).
[33] I. Belabbas, M. A. Belkhir, Y. H. Lee, A. Béré, P. Ruterana, J. Chen, and G. Nouet, Comput. Mater. Sci. **37**, 410 (2006).
[34] J. P. Hirth and J. Lothe, *Theory of dislocations* (Wiley, New York, 1982).
[35] R. de Wit, J. Res. Natl. Bur. Stand. **77A**, 608 (1973).
[36] A. Béré, J. Chen, P. Ruterana, A. Serra, and G. Nouet, Comput. Mater. Sci. **24**, 144 (2002).
[37] L. Verlet, Phys. Rev. **159**, 98 (1967).
[38] C. J. Fall, R. Jones, P. R. Briddon, A. T. Blumenau, T. Frauenheim, and M. I. Heggie, Phys. Rev. B **65**, 245304 (2002).
[39] A. T. Blumenau, M. I. Heggie, C. J. Fall, R. Jones, and Th. Frauenheim, Phys. Rev. B **65**, 205205 (2002).
[40] A. F. Wright and J. S. Nelson, Phys. Rev. B **50**, 2159 (1994).
[41] J. Chen, P. Ruterana, and G. Nouet, Mater. Sci. Eng., B **82**, 117 (2001).
[42] J. Elsner, R. Jones, M. I. Heggie, P. K. Sitch, M. Haugk, T. Frauenheim, S. Oberg, and P. R. Briddon, Phys. Rev. B **58**, 12571 (1998).
[43] S. J. Rosner, E. C. Carr, M. J. Ludowise, G. Girolami, and H. I. Erikson, Appl. Phys. Lett. **70**, 420 (1997).
[44] E. G. Brazel, M. A. Chin, and V. Narayanamurti, Appl. Phys. Lett. **74**, 2367 (1999).
[45] N. Yamamoto, H. Itoh, V. Grillo, S. F. Chichibu, S. Keller, J. S. Speck, S. P. DenBaars, U. K. Mishra, S. Nakamura, and G. Salviati, J. Appl. Phys. **94**, 4315 (2003).
[46] W. T. Read, Philos. Mag. **45**, 775 (1954).
[47] H. J. Im, Y. Ding, J. P. Pelz, B. Heying, and J. S. Speck, Phys. Rev. Lett. **87**, 106802 (2001).
[48] N. G. Weinmann, L. F. Eastman, D. Doppalapudi, H. M. Ng, and T. Moustakas, J. Appl. Phys. **83**, 3656 (1998).